JOURNAL OF PROTEOMICS 112 (2015) 125–140

Available online at www.sciencedirect.com

ScienceDirect

www.elsevier.com/locate/jprot

Cellular and proteomics analysis of the endomembrane system from the unicellular *Entamoeba histolytica*

Doranda Perdomo[a,b,c,1], *Nawel Aït-Ammar*[a,b], *Sylvie Syan*[a,b], *Martin Sachse*[d], *Gagan Deep Jhingan*[e], *Nancy Guillén*[a,b,*]

[a]*Institut Pasteur, Cell Biology of Parasitism Unit, F-75015 Paris, France*
[b]*INSERM U786, F-75015 Paris, France*
[c]*Université Paris Diderot, Sorbonne Paris Cité, Cellule Pasteur, F-75015 Paris, France*
[d]*Institut Pasteur, Imagopole, Plate-Forme de Microscopie Ultrastructurale, France*
[e]*National Institute of Immunology, Aruna Asaf Ali Marg, New Delhi, India*

ARTICLE INFO

Article history:
Received 21 February 2014
Accepted 18 July 2014
Available online 7 August 2014

Keywords:
Traffic
Endomembrane system
Entamoeba

ABSTRACT

Entamoeba histolytica is the protozoan parasite agent of amoebiasis, an infectious disease of the human intestine and liver. Specific active pathogenic factors are secreted toward the external milieu upon interaction of the parasite with human tissue. Trafficking dynamics and secretion of these factors is not known and characterization of the dynamics interplay of subcellular compartments such as the ER or Golgi apparatus is still pending. In this work, we took advantage of cell fractionation and a wide proteomic analysis to search for principal components of the endomembrane system in *E. histolytica*. Over 1500 proteins were identified and the two top categories contained components of trafficking machinery and GTPases. Trafficking related proteins account for over 100 markers from the ER, Golgi, MVB, and retromers. The lack of important components supporting Golgi polarization was also highlighted. The data further describe principal components of the endosomal traffic highlighting Alix in isolated vesicles and during parasite division.

Biological significance
This work represents the first in-depth proteomics analysis of subcellular compartments in E. histolytica and allows a detailed map of vesicle traffic components in an ancient single-cell organism that lacks a stereotypical ER and Golgi apparatus to be established.

1. Introduction

Trafficking pathways between organelles are highly conserved between mammalian, plant, and yeast cells. The vesicular transport hypothesis states that the transfer of cargo molecules between organelles of the secretory pathway is mediated by shuttling transport vesicles. This means that a donor compartment (vesicle budding) buds by a selective

DOI of original article: http://dx.doi.org/10.1016/j.dib.2014.08.007.
* *Corresponding author at:* Cell Biology of Parasitism Unit, Institut Pasteur, 28 rue du Dr Roux., 75724 Paris Cedex 15, France. Tel.: +33145688675; fax: +3145688674.
E-mail addresses: doranda.perdomobastidas@mail.mcgill.ca (D. Perdomo), nguillen@pasteur.fr (N. Guillén).
[1] Present address: Doranda Perdomo, CFTR Research Center, Physiology Department, McGill University, Montreal, Canada.

http://dx.doi.org/10.1016/j.jprot.2014.07.034

process for the incorporation of cargo into the forming vesicles while retaining resident proteins in the donor compartment (protein sorting). The vesicles are subsequently targeted to a specific acceptor structure (vesicle targeting), into which they unload their cargo upon fusion of their limiting membranes (vesicle fusion). All of these steps are regulated so that a large amount of cargo can be transported without compromising the integrity or composition of the known organelles: Endoplasmic reticulum (ER), Golgi apparatus, lysosomes, early endosomes, and multivesicular bodies (MVB).

Typically, the ER is organized into branching tubules and flattened sacs that are interconnected, and comprised of a nuclear envelope, membrane sheets, tubules and cisternae [1]. It is a highly dynamic structure within the diverse eukaryotic cells; where the global morphology of the ER is well conserved as well as its cargo and lipid secretory mechanisms [2]. The Golgi apparatus, responsible for receiving, processing, and sorting newly synthesized proteins and lipids through the secretory pathway, consists of four to six flattened micron-sized membrane-bound cisternae arranged as a stack with surrounding vesicles and fenestrated margins that can take the form of tubules and tubular networks [3]. According to the species being studied, the morphology of the Golgi apparatus can differ. It can be organized as individual cisternae in *Saccharomyces cerevisiae* [4], as single stacks in plants [5] and parasites such as *Trypanosoma brucei* [6], or as pairs of stacks in *Drosophila* [7]. Biochemically, several models have been proposed to explain the protein and lipid sorting through the Golgi apparatus [8]. Overall, they share some principal steps, with the first taking place in earlier (cis) cisternae, where proteins arrive from the ER and the last steps at later (trans) cisternae, where cargo departs for the plasma membrane and other post-Golgi destinations. In between, COPI vesicles bud from Golgi cisternae [9], SNAREs (soluble N-ethylmaleimide-sensitive factor attachment protein receptors) mediate specific membrane fusion [10], BAR and related proteins create tubular networks [11], Rab proteins create functional domains within a single membrane [12], and vesicles are tethered at target membranes [13].

In the parasite *Entamoeba histolytica*, the causative agent of amoebiasis, an interesting aspect of its cellular biology is that this single-celled organism lacks visible classical organelles such as mitochondria and rough ER although it has Golgi/ER associated functions [14–16] and contains remnant mitosomes where the major function in *E. histolytica* is that of sulfate activation [17]. Initial studies through cellular fractionation revealed the ER marker BiP (heat shock protein 70-related) present in the endomembrane system of *E. histolytica* [16]. Furthermore, calreticulin, another ER protein marker, is found in cytotoxic complexes such as uropod caps [18], and within phagocytic-structures [19] providing a possible link between the pathogenesis process and the localization of certain ER protein markers. Resident luminal ER proteins containing the KDEL sequence motif are retained in the lumen of the ER [20]. Using the green fluorescent protein (GFP) and the KDEL retrieval motif [16], the presence of a continuous ER compartment has been suggested. More recently, it was found that nitric oxide, an intracellular messenger known to be one of the most versatile players in the immune system, dramatically provokes extensive ER fragmentation in *E. histolytica* [21]. Proteins are translocated into the ER lumen or integrated into the ER membrane through a channel formed by the heterotrimeric Sec61 complex, which is formed by subunits α, β, and γ. The Sec61α subunit has been identified in *E. histolytica* where it shows an irregular staining pattern throughout the cytoplasm and is also found on the cell surface. Sec61α downregulation affects cell proliferation, subcellular distribution of two virulence factors, and the ability of the trophozoites to cause liver abscess in hamsters [22]. In addition, two ER protein markers, ERD2 (ER luminal protein receptors) which mediated retrograde transport and PDI (protein disulfide isomerase) exhibit a redistribution in the cytoplasm upon interaction with Brefeldin A (BFA), a fungal metabolite that causes the redistribution of Golgi proteins to the ER and the subsequent collapse of the Golgi stacks [23].

Important proteins with homology to the Golgi mammalian system have been described in *Entamoeba*, such as the N-ethylmaleimide-sensitive factor (NSF), which is responsible for the disassociation of SNARE complexes after fusion with the target membranes by ATP hydrolysis [24]. The NSF protein shares a 40% homology with human NSF and has ATPase activity and intra-Golgi transport activity in vitro. In addition, the gene homologues of SNAP, t-SNARE, and v-SNARE were also identified in the *E. histolytica* genome databases. The data implies that the parasite contains the essential components for vesicle trafficking and fusion, which has yet to be fully described. Further analysis of the amoebic genome identified an unusual high number of genes encoding Ras-related proteins from the small GTPase family exceeding those of mammals or plants dedicated to vesicular sorting [25]. These genome predictions suggest that endosome/exosome trafficking functions may be highly active in *E. histolytica*. For example, the diversity and complexity of Rab proteins present in *E. histolytica* likely reflect vigorous and dynamic membrane transport and reliance on Rab proteins for vesicular trafficking specificity [25]. Specifically, two Rab proteins, Rab5 and Rab7A, have been identified and are associated with the phagosomal cup during engulfment of human cells, a characteristic process for *E. histolytica*. A subset of proteins known as the vacuolar protein sorting (Vps) in yeast that interact with these Rab proteins was also identified during phagocytosis and include: Vps26p, Vps35p, and Vps29p [26,27] as well as Vps4p, an ATPase ESCRT protein associated with the cytopathic activity of *E. histolytica* [28].

E. histolytica possesses a high content of vesicles, although the mechanism of vesicle sorting and secretion that plays an important role in the delivery of pathogenic factors to human cells is so far unknown. Therefore, this work focused on the characterization of the internal membranes from *E. histolytica* by proteomics. Electron microscopy demonstrates that the internal membrane fraction contains vesicles and vacuoles with a delimiting membrane with some electron dense content. Our detailed proteomic analysis of the endomembrane system identified proteins relevant to the ER, vesicle translocation, sorting, glycosylation and components of the Golgi, endosomes, and MVBs. Vesicle fusion proteins such as COPI and II components and SNARES were found and the newly identified Alix-like protein, all of which are relevant to the endosomal sorting and traffic pathway. Relevant cargo molecules including main virulence factors were found to be associated with the

endomembrane fraction. Abundance of some identified factors, absence of important Golgi markers, and discovery of new proteins essential for vesicular transport provide an intricate picture of vesicular transport in *E. histolytica*.

2. Materials and methods

2.1. Cell strains and culture

The axenic *E. histolytica* strain HM1:IMSS was cultivated in TYIS-33 medium at 37 °C [29].

2.2. Cell fractionation

E. histolytica subcellular fraction separation was performed as described before [30] with some modifications. A trophozoite pellet corresponding to 2×10^8 cells was resuspended in 10 mM $MgCl_2$ and 10 mg Concanavalin A (ConA, Sigma) with a 5 minute incubation on ice. Then, the solution was centrifuged at 500 *g* to eliminate the excess of ConA. The pellet was resuspended in 10 mM Tris–HCl buffer with 1 mM $MgCl_2$ and 2 mM AEBSF and left on ice for 10 min. Trophozoites were then lysed by a glass Dounce Homogenizer (18 to 20 strokes). The solution obtained was added to a sucrose–manitol gradient (0.58:0.50 M) and centrifuged 30 min at 250 *g*. The pellet (C1) corresponded to membranes and the supernatant (S1) corresponded to vesicles and cytoplasm. The S1 fraction was centrifuged at 40 000 *g* for 1 h in order to collect the vesicles in the pellet C2. The supernatant from this last fraction, S2, corresponded to the cytoplasm. The vesicle fractionation was performed as previously described [31]. Basically, the C2 fraction was resuspended in a 10 mM Tris–HCl buffer with 0.25 M of sucrose, 1 μg/ml leupeptin, 1 mM DTT, and 0.5 mM AEBSF, and the sum added to a sucrose gradient (38%, 30%, 25%, and 15%) for centrifugation at 170 000 g for 1 h. Each pellet collected was then centrifuged again at the same speed and time.

The C1 fraction was then resuspended in 10 mM Tris–HCl with 1 M methyl–mannoside and incubated for 30 min on ice. The solution was then centrifuged for 10 min at 250 *g*. The pellet was resuspended in the previous buffer with a ratio of 1:3 Tris–HCl and 1 M methyl–mannoside, and then homogenized and added to a 20% sucrose solution and centrifuged for 30 min at 250 g. The supernatant was centrifuged for 1 h at 40 000 g. The pellet obtained contained the membranes and was resuspended in 10 mM Tris–HCl with protease inhibitors and kept at −20 °C until further use. The internal membrane and plasma membrane fractions were controlled by western blots for the presence of CRT (with and amoebic specific anti-CRT (1:200 [18])), for NSF (with a monoclonal anti-NSF 1:50; Santa Cruz clone E6), the lysine and glutamic rich protein KERP1 (monoclonal antibody C2-7, our laboratory) and the heavy chain of the Gal/GalNAc lectin (polyclonal antibody, our laboratory).

2.3. High pressure freezing and freeze substitution for transmission electron microscopy (TEM)

Trophozoites were concentrated by centrifugation at 600 g. The pellet was carefully resuspended and the suspension was taken up in capillary tubes (Leica, Vienna, Austria) as described [32]. The filled tube was separated by clamping into segments of less than 2 mm and placed into the 200 μm deep cavity of a brass planchette, Type A (Agar Scientific, Stanstad, England) filled with 1-hexadecen. With the flat side of the complementary Type B planchette the filled planchette was closed and frozen with the HPM 010 (Baltec, now Abra Fluid, Wichau, Switzerland).

Freeze-substitution was performed in anhydrous acetone (EMS, Hatfield, USA) containing 1% osmium tetroxide (Merck, Darmstadt, Germany). 1-Hexadecen is insoluble at −90 °C in dry acetone. For the substitution mix to access the sample, small cracks were introduced under liquid nitrogen in the solid hexadecen by application of gentle pressure with pre-cooled fine point forceps (#5, Dumont, Switzerland). Substitution was done at −90 °C for 24 h, and at −60 °C and −30 °C for 8 h each in an automated substitution device (Leica AFS, Leica Microsystems, Vienna, Austria). Next, the temperature was raised to 0 °C and the samples were washed with dry acetone and embedded stepwise in Epon. Thin sections were cut with an Ultracut UCT microtome (Leica Microsystems, Vienna, Austria). Sections were collected on 200 mesh formvar coated copper grids and poststained with 4% uranyl acetate and Reynold's lead citrate. Images were taken with a Jeol 1010 at 80 kV with a KeenView camera (Olympus, Soft Imaging Systems, Münster, Germany).

2.4. Immunolabeling of the endomembrane fraction for TEM

10 μl of the endomembrane fraction were adhered to the 200 mesh formvar coated copper grids for 20 min at RT. After a brief rinse in 0.1 M Hepes, pH 7.4, the sample was fixed with 4% paraformaldehyde in 0.1 M Hepes for 20 min. Next, free aldehydes were quenched with 50 mM NH_4Cl in PBS before incubation with the rabbit anti-Alix antibody. The bound antibody was visualized with protein A gold (10 nm, CMC Utrecht, The Netherlands). Grids were contrasted using 0.4% uranyl acetate in 1.8% methylcellulose.

2.5. Localization of proteins by immunofluorescence in *E. histolytica*

Trophozoites were grown for 48 h as previously described on glass coverslips. Parasites were washed in Dulbecco's Phosphate Buffer (DPBS) and then fixed with 4% methanol-free formaldehyde for 30 min at 37 °C then washed with 0.1 M glycine DPBS and permeabilized with 0.5% Triton X-100 for 2 min. Samples were blocked with 3% BSA–DPBS for 1 h. The samples were labeled with an amoebic specific anti-CRT (1:200 [18]), a monoclonal anti-NSF (1:50; Santa Cruz clone E6), a rabbit polyclonal anti-Alix (1:200; prepared for this work). For secondary antibodies, goat anti-rabbit Alexa Fluor 488 antibody or goat anti-rabbit Alexa Fluor 546 antibody, respectively (1:200; Molecular Probes) were used. Coverslips were washed again in PBS and mounted with ProLong antifading reagent containing DAPI (Molecular Probes). Images were acquired in Z-stacks with an LSM700 confocal microscope (Zeiss). To prepare anti-Alix specific antibodies the following peptides ^{707}NPPPLQENNTSKPYP and ^{775}TVSKSNQPVNRYPTT from the Alix (EHI_167710) sequence were injected together

into two rabbits according to protocols of a private company (Eurogentec, Belgium), sera were recovered upon three immunization steps.

2.6. Preparation of samples for proteomics analysis

Proteins from the internal membrane fraction (50 μg) were precipitated with the methanol–chloroform method [33] and the resulting dried pellet was dissolved in freshly prepared digestion buffer (8 M urea in 25 mM NH_4HCO_3). Samples were reduced with 5 mM TCEP (45 min, 37 °C) and alkylated with 50 mm iodoacetamide (60 min, 37 °C) in the dark. Samples were diluted with 25 mM NH_4HCO_3 to a final concentration of 1 M urea and digested overnight at 37 °C with sequencing grade trypsin gold (1 μg, Promega, USA). After digestion, peptide mixtures were acidified to pH 2.8 with formic acid and desalted with minispin C18 columns (Nestgrp, USA). Samples were dried under vacuum and resolubilized in 0.1% formic acid and 2% acetonitrile before mass spectrometric analysis.

2.7. Liquid chromatography–mass spectrometry (LC–MS/MS) analysis of proteins

The tryptic peptide samples (1 μl roughly containing 1 μg) were separated by reverse-phase chromatography for each experiment via Thermo Scientific Proxeon nano LC using a C18 picofrit analytical column (360 μm OD, 75 μm ID, 10 μm tip, Magic C18 resin, 5 μm size, Newobjective, USA). The HPLC was coupled to an LTQ-Orbitrap Velos mass spectrometer (Thermo Fisher Scientific). Peptides were loaded onto the column with Buffer A (2% acetonitrile, 0.1% formic acid) and eluted with 120 min linear gradient from 2 to 40% buffer B (80% acetonitrile, 0.1% formic acid). After the gradient the column was washed with 90% buffer B and finally equilibrated with buffer A for the next run. The mass spectra were acquired in the LTQ Orbitrap Velos with full MS scan (RP 30000) followed by 10 data-dependent MS/MS scans with detection of the fragment ions in the FTMS HCD mode (RP 7500). Target values were 1×10^6 for full FT-MS scans and 5×10^4 for FT-MS MS*n* scans. The ion selection threshold was set to 5000 counts.

2.8. Proteomic data analysis

Data analysis was performed using Thermo Proteome Discoverer software suite (version 1.4). For the search engine SEQUEST, the peptide precursor mass tolerance was set to 10 ppm, and fragment ion mass tolerance was set to 0.6 Da. Carbamidomethylation on cysteine residues was used as fixed modification, and oxidation of methionine along with N-terminal acetylation was used as variable modifications. Spectra were queried against the *E. histolytica* UniProt database. In order to improve the rate of peptide identification percolator node in Proteome Discoverer was utilized with the false discovery rate (FDR) set to 1% for peptide and protein identification.

In order to determine the absolute abundance of different proteins within a single sample we used iBAQ feature of MaxQuant version 1.4.0.5 software using default search parameters [34,35]. The results of Proteome Discoverer and MaxQuant searches were arranged together. The mass spectrometry proteomics data have been deposited to the open access library of the ProteomeXchange Consortium (http://www.proteomexchange.org) via the PRIDE partner repository [36] with the dataset identifier PXD000770.

2.9. Bioinformatic analysis

Proteome Discoverer annotation node, which is connected to the ProteinCenter web based application, was used to download categorical GO database information in the form of biological process (BP), molecular function (MF), and cellular component (CC). MaxQuant and Perseus were utilized for protein identification and assignment of Interpro, KEGG, and Prosite annotations along with their iBAQ values.

3. Results

3.1. Morphological analysis of endomembrane structures in *E. histolytica*

To illustrate the diversity of vesicular structures in *E. histolytica*, trophozoites were prepared for transmission electron microscopy analysis by high pressure freezing and freeze substitution (Fig. 1). The fast immobilization of high pressure freezing together with the dehydration in the cold during freeze substitution results in better morphological preservation, compared to chemical fixation and dehydration at room temperature. The overview of the cell shows several big vacuoles present in the cytoplasm. These vacuoles are characterized by an electron lucent lumen and few internal membranes. Next to those vacuoles, large vacuoles with an electron dense lumen consisting of membranous sheets and amorphous material can be found. In addition, many vesicles of diverse diameters and long tubular profiles are found in the cytoplasm of the trophozoites. Tubular profiles are either present with an electron lucent or a more dense lumen. Occasionally the static EM image catches a vesicle budding or fusion event that could be implicated in the trafficking between the different compartments.

In order to identify and initiate the characterization of the protein sorting routes in *E. histolytica*, we began by pinpointing the subcellular sites of calreticulin (CRT) and NSF. CRT has been previously shown to be present throughout the cytoplasm, adjacent to the nuclei, and close to the plasma membrane [16]. CRT localization by confocal imaging confirmed these previous data indicating a morphological undefined ER (Fig. 2A). NSF, a protein responsible for dissociating SNARE complexes after their fusion with target membranes [37] (i.e. Golgi, endosomes and plasma membrane) was localized diffusely in the cytoplasm and was viewed as small dots (Fig. 2A). CRT and NSF do not colocalize, indicating that these two markers do not associate in a particular compartment.

3.2. Proteomic analysis of subcellular compartments in *E. histolytica*

3.2.1. Fractionation of subcellular compartments of *E. histolytica*

To perform a subcellular fractionation of *E. histolytica* endomembranes we applied a previously described technical

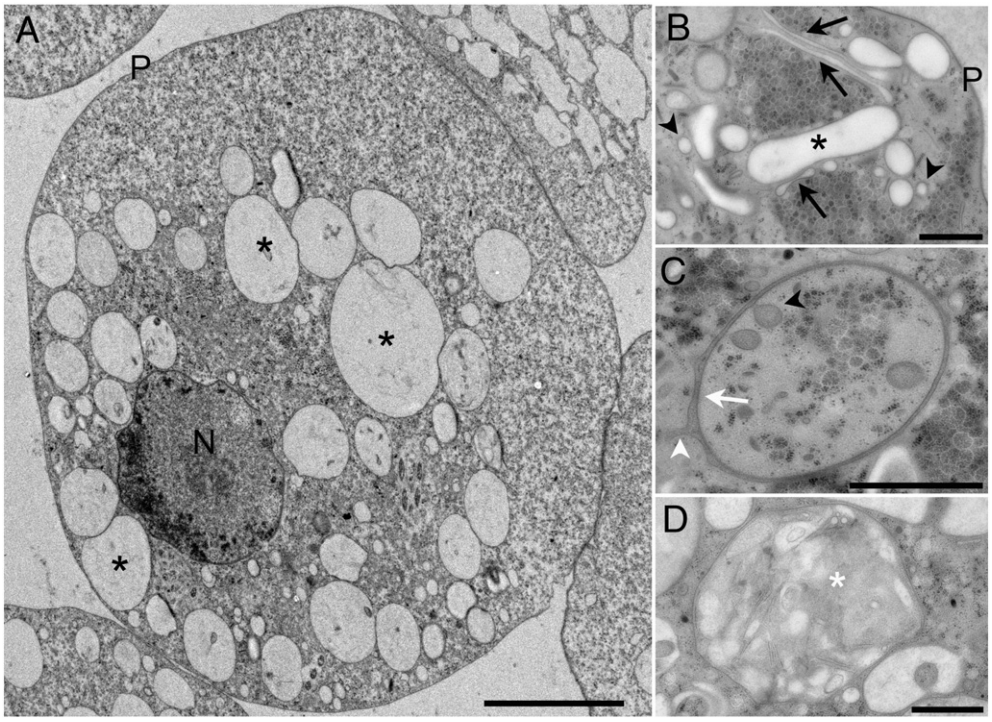

Fig. 1 – *Entamoeba histolytica* has a complex and diverse endomembrane system. Trophozoites were prepared for TEM analysis by high-pressure freezing and freeze substitution. (A) Shows an overview of *E. histolytica* with the plasma membrane (P) outlined. Within the cytoplasm many vacuoles of different sizes are present (examples marked by asterisks). (B–D) Endomembrane system details. (B) Besides vacuoles with an electron lucent lumen (asterisk), tubular profiles (black arrows), and vesicles (black arrowheads) are distributed throughout the cytoplasm. (C) Tubular profiles (white arrow), branch (white arrowhead), or a budding/fusion event with a vesicle (black arrowhead). (D) A subset of vacuoles (white asterisk) contains amorphous, electron dense material and internal membranes. Scale bars: (A) = 5 μm; (B–D) = 1 μm.

approach [30]. This procedure using mannitol and sucrose gradients sorts the proteins into three main compartments: plasma membrane, internal membranes, and cytoplasm. Using specific antibodies recognizing either CRT or NSF, we examined by immunoblotting the eventual presence of both markers in the diverse fractions from the subcellular separation (Fig. 2B). CRT (50 kDa) was enriched in the internal membrane fraction and was less abundant in the plasma membrane associated compartment (Fig. 2B). NSF (75 kDa) was only found in the internal membrane fraction. To control the protein loading in the plasma membrane fraction from which NSF was absent, KERP1 [38] and Gal/GalNAc (Fig. 2B) were used. Analysis of the internal membrane fraction by electron microscopy showed vesicles of different shapes with sizes ranging from 50 to 200 nm (Fig. 2C). Further fractionation of the internal membrane compartment was attempted by sucrose gradient separation [31]. Unfortunately (data not shown), the presence of CRT was detected in all individual sub-fractions upon western blot analysis, indicating that an enrichment of the ER was not obtained. NSF was not observed suggesting that it was degraded and/or dissociated from the endomembranes. As in other systems isolation strategies of the Golgi have been tricky and therefore purity is limited when using sucrose density centrifugation strategies [39].

3.2.2. Analysis of internal membrane faction of E. histolytica by LC–MS/MS

The population of vesicles ranging from 50 to 200 nm in size obtained within the internal membrane fractions provided us with an ideal opportunity to identify novel and unknown trafficking proteins at a system-wide level. Internal membrane compartments represent a mixture of several membrane fractions localizing CRT and NSF. The interest on this fraction is due to the fact that levels of plasma membrane proteins are highly reduced. Surface proteins are indeed present although expected at low levels [30] since these maybe also components of intracytoplasmic membranes network, this is due to the intense membrane invaginations and vesicle turnover within intracellular compartments of *E. histolytica*.

Protein fractions were prepared from three independent biological experiments and processed for proteomics analysis. We utilized high resolution proteomics technology along with bioinformatic approaches to identify and annotate all the identified proteins into various functional classes. We undertook this proteomics analysis in order to distinguish ER- and Golgi-resident proteins as well as markers of diverse vesicle trafficking pathways. The procedure will give less insight on soluble proteins temporarily interacting with those subcellular compartments. The LC–MS/MS analyses of all three

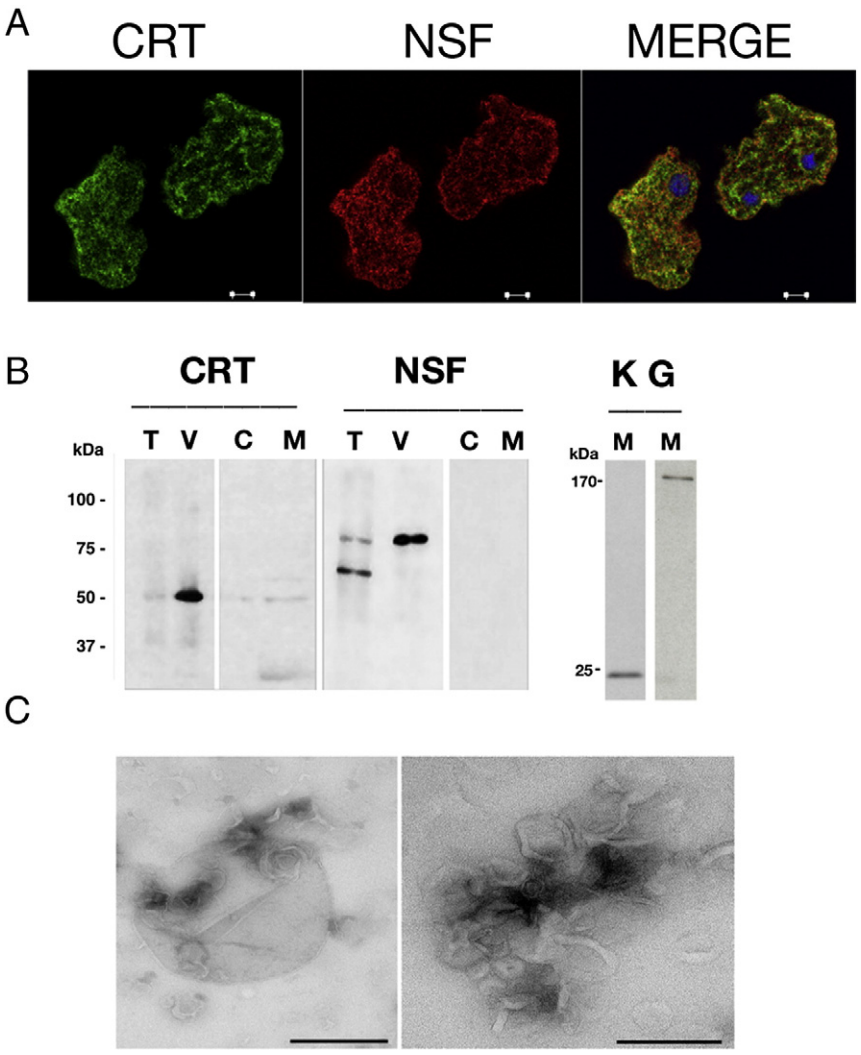

Fig. 2 – Cellular and biochemical analysis of endomembrane fraction from *E. histolytica*. (A) Cellular localization of N-ethylmaleimide sensitive fusion protein (NSF) and calreticulin (CRT) was performed by labeling the parasites with either an anti-NSF (red) or an anti-CRT antibody (green) and nuclei was stained with DAPI (blue). Confocal imaging micrograph is from a focal plane at the middle of the cells demonstrating that NSF and CRT are distributed throughout the cytoplasm in defined small vesicles. Scale bar = 10 μm. (B) Localization of CRT (55 kDa) or NSF (75 kDa) in the subcellular fractions corresponding to total (T), internal vesicles (V), cytoplasm (C), and plasma membranes (M), obtained as published [30]. Positive quality control of the plasma membrane fraction is shown by detection of KERP1 (K at 21 kDa) as published before [38] or Gal/GalNAc heavy chain (G at 170 kDa). (C) Electron micrograph of isolated internal membranes. Scale bar = 200 nm.

biological samples were performed using the LTQ-Orbitrap Velos mass spectrometer in high-resolution MS1 and MS2 modes (MS and MS/MS at 30000 and 7500 resolution with HCD fragmentation) resulting in excellent quality fragmentation spectra providing increased specificity during database searching. For peptide and protein identification, the raw data files were screened using both the Proteome Discoverer and MaxQuant software against the *E. histolytica* Uniprot database. The entire dataset is in open access (ProteomeXchange library identifier PXD000770). Due to existing diverse gene annotations for *E. histolytica*, we kept the largest protein list given by Uniprot, which assembles all the proteins identified in *E. histolytica* independently of the way that it was used for such identification (i.e., prediction from the genome, experimental data); consequently some of these entries should be redundant and may concern the same protein. Using a peptide and protein FDR of 1%, a total of 5683 peptides matching with 1531 proteins (representing 1198 groups) were identified among the three internal membrane samples which corresponds to roughly 20% of the total amoebic proteome. *Details of this analysis can be found in Data in Brief from the Journal of Proteomics.*

Further bioinformatic investigations searching for domain homologies (Smart and InterProScan programs) and functional descriptions (KEGG and GO terms) allowed this data to be organized into distinct categories (Fig. 3). From these categories, 481 proteins were related to vesicle traffic, small GTPases, cargo molecules and enzymes related to ER compartment activities. Proteins related to the ER, endosomes and MVBs are the most represented proteins within the trafficking category with 51, 24, and 25 entries, respectively (Fig. 3C). We

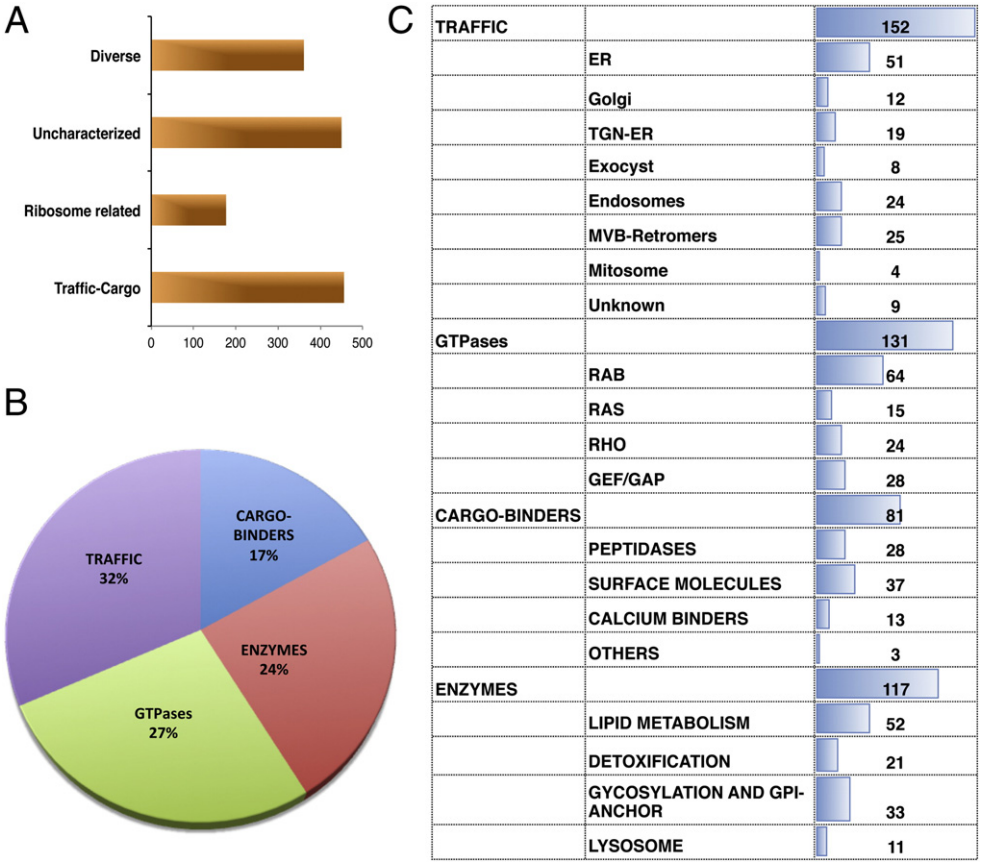

Fig. 3 – Proteins identified by LC–MS/MS with their corresponding categories. (A) Categories represented among the proteins identified in the isolated internal membrane fraction. (B) Percentage of proteins related to endomembrane compartments. (C) Specificity of proteins identified in the traffic category.

identified 12 entries related to the Golgi apparatus and associated proteins and 19 entries related to the TGN–ER retrograde transport that can be associated with 8 exocyst-related categories (Fig. 3C) whereas 9 of unknown function present domains related to Golgi and HEAT domain involved in intracellular transport.

In addition to protein identification, we utilized the Intensity-based absolute quantification (iBAQ) method to measure protein abundances within the three biological samples after calculating the median iBAQ values. After applying the iBAQ algorithm on the three raw files (containing 1531 proteins), 1015 proteins had measurable iBAQ values. The iBAQ values varied over 5 orders of magnitude with respect to the most abundant and least abundant proteins (Fig. 4A). Proteins related to the ER, Golgi, and ribosomal families were present among the 25 most abundant proteins while the 25 lowest abundance proteins were related to general cellular process (Fig. 4B, C). Overall, the iBAQ analysis showed calreticulin to be the most abundant protein among all 1531 identified proteins of the internal membranes from *E. histolytica*.

3.2.3. *Proteins related to the endoplasmic reticulum*

As illustrated in Fig. 3C, the principal ER constituents identified in this analysis are from the translocon machinery necessary for proteins to be transported from the ribosomes to and/or across the ER membrane or to be integrated into the ER membrane (Fig. 5). Sec61 comprises the main protein-conducting channel, whereas signal-recognition particle receptor (SRPR), signal peptidases (SPC), the translocon associated protein complex (TRAP), Sec63, and BIP comprise associated proteins that assist in signal sequence-mediated targeting, cotranslational translocation, and processing of nascent polypeptide chains. The conducted proteomics analysis identified SRPRα, SRPRβ, SPC2, SPC3, TRAPβ, Sec61α, Sec61γ, and BIP (Hsp70). Sec63 was not identified, although a gene encoding this protein is present in the amoebic genome (Fig. 5).

In the ER related category, we also found chaperones from the heat shock family (Hsp70 and Hsp90), calreticulin, and important enzymes involved in lipid biosynthesis, GPI anchor biogenesis, and glycosylation processes. Sequence homology analysis showed conservation of Hsp protein domains within the 26 identified candidates (Supplementary Fig. 1). Among them, three (C4M5K9, C4M770 and O77164) display a canonical KDEL ER-retention motif at their carboxyl-terminal end whereas C4LT65 carries a KTEL divergent motif. In the further analysis, we concentrated on protein components of vesicles carrying cargo from the ER to the Golgi: COPII (coat protein complex II)-coated vesicles.

COPII-coated vesicles form on the ER by the sequential recruitment of three cytosolic components: (i) GTPase Sar1, a membrane bending protein that is important for the initiation of coat formation; (ii) Sec23/Sec24, a heterodimer that is

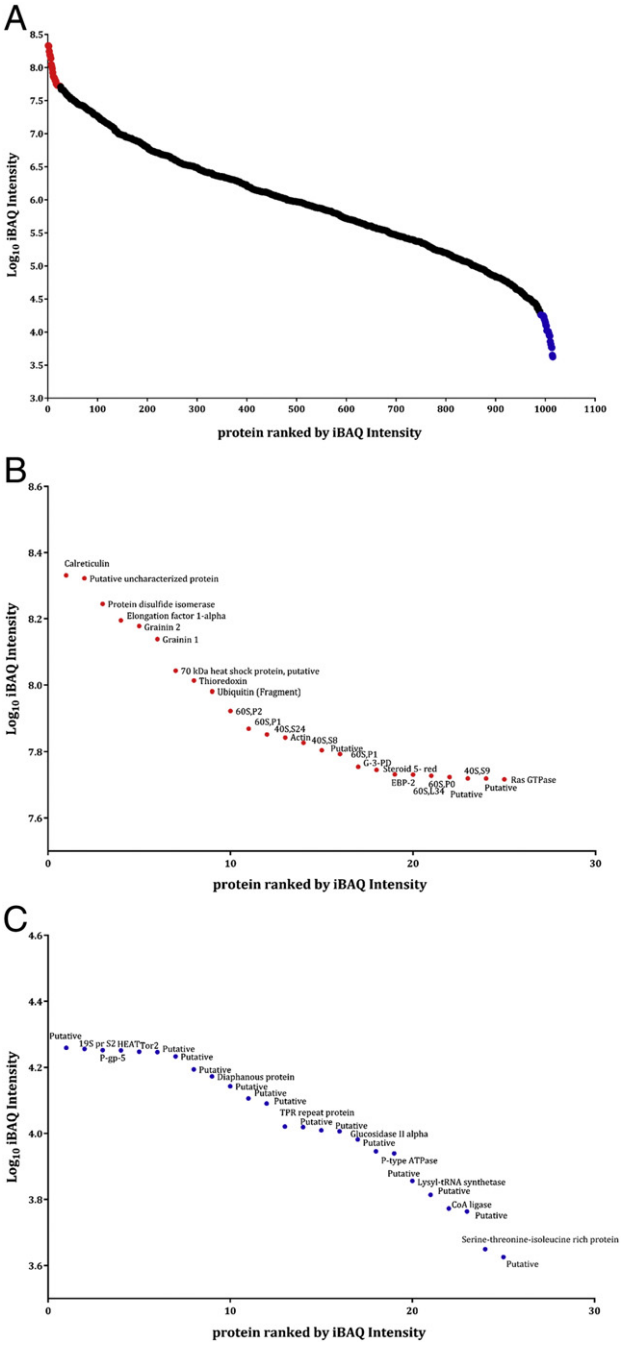

Fig. 4 – Dynamic range of internal membrane proteome from *E. histolytica*. (A) S-shaped distribution of median absolute expression values of 1015 iBAQ quantifiable proteins. For all proteins, iBAQ values reveal a dynamic range of abundance at a magnitude of five orders. (B) The 25 most abundant proteins consist of ER, Golgi, and ribosomal-related proteins. (C) The set of 25 proteins with the lowest abundance contains general cellular proteins.

necessary for the capture of cargo proteins into nascent buds; and (iii) Sec13/Sec31, which is involved in coat polymerization and membrane deformation. Sec13, Sec31, Sec23 and Sec24 were identified in the proteomic analysis, whereas Sar1 was not identified, but is predicted from the genome annotation. We identified members of the p24 family of proteins (p24, gp25L, emp24, Erp), which are receptors within COPII vesicles for cargo molecules transported from the ER to the Golgi complex. All identified emp24 family members carry the GOLD domain (for Golgi dynamics) that is present in lipid-trafficking proteins [40]. In addition, we found Sedlin, a subunit of the transport protein particle (TRAPP) complex involved in the targeting and fusion of endoplasmic reticulum (ER)-derived transport vesicles to the Golgi acceptor compartment. Finally, we detected two proteins sharing homology with SEY1, which in *S. cerevisiae* is involved in membrane trafficking and in *Arabidopsis thaliana* (RHD3 proteins) mediates ER fusion and the formation of the tubular ER network.

3.2.4. *Proteins related to the Golgi apparatus and TGN–ER retrograde transport*

Besides COPII transport from ER to Golgi, COPI transports cargo within the Golgi and from the Golgi to ER. The coat protein complex I (COPI) consists of a heptameric (α, β, β′, γ, δ, ε, ζ) complex, also called coatomer, with two main subcomplexes: (i) the γ,δ,ζ,β-COP tetrameric complex, which constitutes the inner layer core; and (ii) the α,β′,ε-COP trimeric complex, which forms the outer layer of the COPI coat. COPI vesicles are generated through Arf1, a regulatory GTPase, activation at the donor membrane and the subsequent recruitment of coatomer, which functions in binding and sequestering cargo molecules. With the exception of ε-COP, we identified all components of COPI including Arf1.

Cargo movement through the Golgi depends on vesicle fusion and scission; although the pathway in Golgi transport is a debatable theme [8], an important and constant feature involves soluble NSF-attachment proteins (SNAPs). These proteins are highly conserved between organisms and participate in intracellular membrane fusion and vesicular trafficking. Three different isoforms of SNAPs have been described, α-, β-, and γ-SNAP [41], with α-SNAP being the most relevant to vesicle trafficking. During membrane fusion, α-SNAP is recruited to the SNARE complex cycle (V- and T-SNARE), where a monomeric V-SNARE (synaptobrevin and SNAP-25) on the vesicle binds to an oligomeric T-SNARE on the target membrane, forming a stable four-helix bundle that promotes membrane fusion [42,43]. A bound α-SNAP complex recruits NSF, thus dissociating the SNARE-complex by ATP hydrolysis [37] and allowing the cycle to progress. In our LC–MS/MS results, we detected the presence of both α- and γ-SNAP proteins in the membrane purified fraction as well as annotated SNARE component synaptobrevin and NSF (Fig. 6). We also identified annotated SNARE complex interactors Syntaxin 1A and B, as well as Syntaxin 16. Syntaxin 1A and B are involved in exocytosis [44] and Syntaxin 16 is involved in endosomal trafficking [45–47]. Exocytic vesicles are generated at the Golgi apparatus and are transported by motor proteins along cytoskeletal tracks and motor proteins to the plasma membrane [48]. Vesicle fusion at the target membrane is facilitated by SNARE proteins present on both the vesicle and target membranes. We distinguish Vps33, a protein that regulates cargo delivery by interacting with SNAREs in early endosomes through the HOP complex [49], and Vps45, an exocytosis protein and a homologue of Sec1 involved in stabilizing the SNARE complex [50]. The composition of the exocyst is highly conserved in eukaryotic systems, with eight

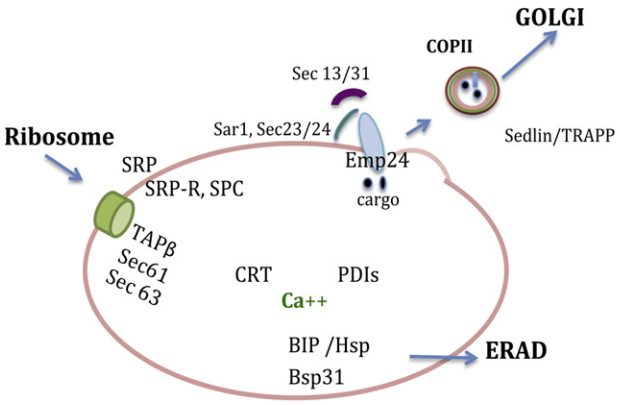

Uniprot	Amoeba DB	Identification
C4M417	EHI_195140	B-cell receptor-associated 31-like
C4M296	EHI_136160	Calreticulin
C4LZG8	EHI_138080	emp24
Q1EQ43	EHI_058320	emp24A
Q1EQ41	EHI_023070	emp24C
Q1EQ40	EHI_038590	emp24D (Fragment)
C4M4L8	EHI_031410	GTP-binding protein SAR1
C4M9H4	EHI_105770	Microsomal signal peptidase SPC subunit 2
C4LY73	EHI_051790	Microsomal signal peptidase SPC
C4M5D2	EHI_121860	Microsomal signal peptidase SPC subunit 3
Q5XWD1	na	Disulfide isomerase
C4MB38	EHI_071590	Disulfide isomerase
C4LTM1	EHI_012280	SEY1 homolog 1
C4M6U3	EHI_054180	SEY1 homolog 2
Q1EQ52	EHI_001050	Transport protein SEC13
Q1EQ51	EHI_103410	Transport protein SEC31
C4M4A8	EHI_048170	Transport protein SEC61 gamma subunit
Q1EQ50	EHI_008730	Sec23A
Q1EQ49	EHI_175480	Sec23B
Q1EQ46	EHI_048310	Sec24C
Q5XWC1	na	Sec61 alpha subunit
C4M5M8	EHI_122820	Sedlin
C4M071	EHI_004750	Signal recognition particle SRP54
C4M3Y9	EHI_200840	Signal recognition particle receptor α subunit
B1N345	EHI_000670	Signal recognition particle receptor β subunit
C4M2Q0	EHI_006160	Signal recognition particle subunit SRP19
C4MB34	EHI_146790	Signal recognition particle subunit SRP68
C4M9X8	EHI_179380	Signal recognition particle subunit SRP9
C4M012	EHI_134630	Translocation protein SEC63
C4M012	EHI_134630	Translocation protein SEC63
C4M944	EHI_083600	Translocon-associated protein beta

Fig. 5 – General scheme of *E. histolytica* ER principal components. According to the LC–MS/MS results and identified proteins, we illustrated a representation of our results coupled with the information found in the literature (blue shadow). Interestingly, we find proteins with roles in the trans Golgi network (TGN) and ER-associated protein degradation (ERAD), as well as ER-resident proteins.

single-copy subunits: Sec3, Sec5, Sec6, Sec8, Sec10, Sec15, Exo70, and Exo84; several of these being identified in the vesicular fraction here examined.

An interesting component of the Golgi apparatus is the golgin proteins that work in Golgi structure maintenance via interaction with small GTPases, the cytoskeleton, and membranes. They serve as an array of loosely associated tentacles providing directional transport between the Golgi and ER [51]. The most identified golgins belong to mammalian organisms with homologues in *S. cerevisiae* or *A. thaliana*. In our hit list we did not find golgin orthologues and after carefully analysis of the *E. histolytica* genome (using Blast and InterProScan), we only found one entry for Golgin A7 (also called GOLGA7 or GCP16), a Ras palmitoyltransferase involved in protein transport from the Golgi to the cell surface [52]. Golgin A7 (C4LT62 at Uniprot) shares 29% identity and 47% homology ($E = 2 \times 10^{-12}$) with human GOG7B (accession no. NP_001010917). However, it is clear from the literature that no single golgin alone can be responsible for maintaining Golgi structure; rather, it is the complex network of interactions between these proteins and their regulators that is important [53].

3.2.5. *Endocytic and vesicular compartment related factors*

The third major class of transport vesicles is the clathrin-coated vesicle (CCV), where clathrin is the predominant protein present in the coat. Clathrin coats use various adaptor complexes to generate vesicles from the trans-Golgi network, endosomes, and the plasma membrane. The connection of the clathrin scaffold to the membrane is mediated by clathrin adaptor (AP) protein complexes. There are 4 different AP coats: AP-1 is involved in TGN to endosomal trafficking; AP-2 in endocytosis at the cell surface; AP-3 in endosomal transport; and AP-4, which is in charge of moving cargo from the TGN toward the plasma membrane [54]. Interestingly, the proteins found in our analysis range from general AP family proteins to specific subunits with homology to AP-1, AP-2, and AP-3, only AP-4 homology was lacking, as it has been shown in other eukaryotic systems [54]. The presence of clathrin coated pits in *E. histolytica* has been previously suggested, specifically for transferrin endocytosis in a mechanism similar to *T. brucei* [55], suggesting a relevant function in this organism.

3.2.6. *Proteins related to multivesicular body function and retromers*

Biological membrane deformation is a major step in getting proteins transported from the Golgi to the ER and the plasma membrane. The process of membrane bending and shape changes is attributed to proteins such as dynamin-like GTPases and proteins processing F-BAR domains [56], which we have detected. These proteins help with vesicle and membrane scission, orchestrating cargo sorting through the clathrin/coatomer vesicle coats (COPI and COPII), as previously discussed, and the endosomal sorting complex required for transport (ESCRT). Early endosomes and MVBs play an important role in sorting endocytosed proteins and newly synthesized lysosomal proteins. In recent years, it was demonstrated that the ESCRT system has a defining role for MVB function in general and protein sorting within the MVB in particular. Specific complexes of ESCRT-I, -II, or -III are identified including Vps (i.e. Vps45, Vps33), Snf7 family protein components, or even Bro protein domains (Alix). In

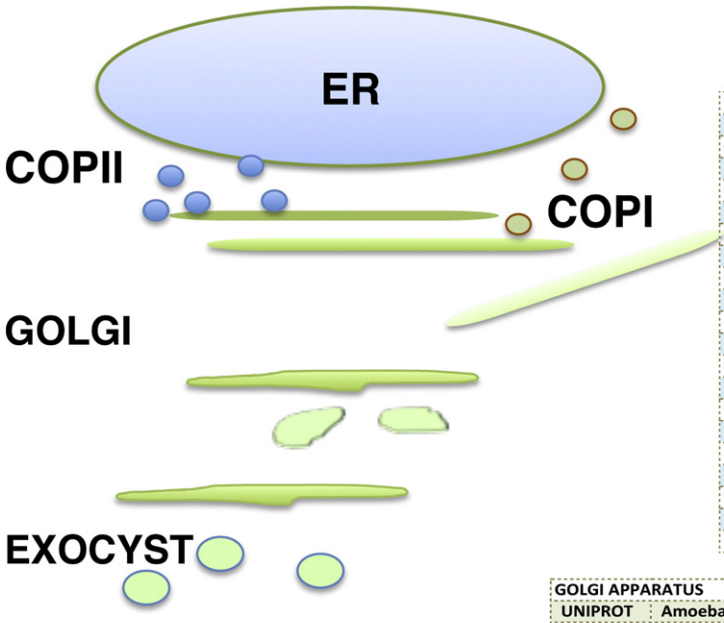

TGN-ER RETROGRADE TRANSPORT

UNIPROT	Amoeba DB	DESCRIPTION
C4LXL1	EHI_073470	ADP-ribosylation factor
Q1EQ57	EHI_194500	ADP-ribosylation factor
Q1EQ59	EHI_073480	ADP-ribosylation factor
Q9NIP7	na	ADP-ribosylation factor (Fragment)
O77162	na	ADP-ribosylation factor (Fragment)
C4LYY9	EHI_118050	Coatomer subunit alpha putative
Q1EQ31	EHI_088090	Coatomer subunit Alpha1
Q1EQ30	na	Coatomer subunit Alpha2
Q1EQ39	EHI_027720	Coatomer subunit beta
Q1EQ38	EHI_088220	Coatomer subunit beta (Fragment)
Q1EQ26	na	Coatomer subunit Beta isoform b
Q1EQ29	EHI_004590	Coatomer subunit Beta prime
Q1EQ37	na	Coatomer subunit Beta3
Q1EQ34	na	Coatomer subunit Delta1
Q1EQ33	EHI_126990	Coatomer subunit Delta2 (Fragment)
Q1EQ35	EHI_012500	Coatomer subunit gamma
Q1EQ36	EHI_040700	Coatomer subunit gamma
Q1EQ24	na	Coatomer subunit Gamma isoform 1
Q1EQ32	na	Coatomer subunit Zeta

EXOCYST COMPLEX

UNIPROT	Amoeba DB	DESCRIPTION
B1N2J9	EHI_068150	Sec8
C4LT29	EHI_148590	Sec3
C4LVV5	EHI_125680	Sec15
C4LW49	EHI_142040	Exo 70
C4M0K1	EHI_024590	Sec7
C4M477	EHI_140290	Sec8
C4M5A1	EHI_081420	Sec6
Q1EPY3	EHI_093130	Sec1

GOLGI APPARATUS

UNIPROT	Amoeba DB	DESCRIPTION
C4M0D4	EHI_064680	Alpha-soluble NSF attachment, a-SNAP
C4M2A1	na	Longin-type vesicle-associated membrane, synaptobrevin
Q1EQ09	EHI_022910	Longin-type vesicle-associated membrane, synaptobrevin
Q5FZL6	EHI_000300	NSF attachment, a-SNAP
Q7Z0T4	na	N-ethylmaleimide-sensitive factor, NSF
B1N344	EHI_136210	Soluble NSF attachment, g-SNAP
Q1EPZ9	EHI_164320	Syntaxin 16 (Fragment)
Q1EQ03	EHI_139030	Syntaxin 1A (Fragment)
C4LT43	EHI_021410	Syntaxin B
Q1EPY7	EHI_106240	Syntaxin E (Fragment)
Q1EQ05	EHI_148750	Syntaxin, putative

Fig. 6 – General scheme of *E. histolytica* TGN-ER principal components. According to the LC–MS/MS results and identified proteins, we illustrated a representation of our results coupled to the information found in the literature. Proteins related to the exocyst complex, retrograde transport from ER-TGN and Golgi apparatus are listed.

the ESCRT-II complex, which is involved in the formation of linear polymers implicated in cargo trapping, membrane deformation, and vesicle abscission, we have identified two members, Vps2 and Snf7 (yeast homologue of Vps32). The ESCRT-III mechanism for vesicle delivery is dependent on Vps4 [57]. Although we did not detect Vps4, we identified proteins (EHI_167710 and EHI_165220) that share homologies with mammalian Alix (a direct interactor with Snf7), which has been found to be necessary for membrane abscission during cytokinesis and virus budding in association with ESCRT-III [58]. Another *E. histolytica* protein identified and characterized with homology to Alix [59] (Fig. 7), is the adhesin protein ADH112 (EHI_181220) that has a role in phagocytosis [60,61] and was found in our analysis. The Alix-homologue (EHI_167710) appeared in all three independent experiments and has differences at the amino acid sequence level (Fig. 7A–B) indicating that in addition to the BRO1 domain (IPR004328), characteristic of the Alix family, it bears specific domains (Fig. 7C). Besides these described MVB components — we also found a high number of related ATPase (i.e. V-type ATPase, vacuolar ATP synthase, and vesicle fusing ATPase), and a BAR/SH3 domain containing protein previously annotated as Hse1 (homologous to STAM1, a component of ESCRT-0), which is useful for membrane bending and curvature [11].

Proteins involved in retrograde transport from the endosomal system to the Golgi were also identified. Specifically, we identified the retromer complex heterodimer VPS35–VPS26, a Golgi localized complex responsible for cargo selection as well as endosome to Golgi retrieval from lysosomes [62], but we did not find VPS29. Interestingly, the *E. histolytica* retromer complex was described to be involved in a phagocytic process, where Rab7A, a protein associated with phagosomal cups in the parasites, was able to pull amoebic retromer complex VPS35–VPS26 and VPS29, implying that the process of lysosomal protease delivery by Rab7A is regulated through the retromer complex [63] or other trafficking processes.

3.2.7. Small GTPases present in the internal membrane fraction

Members of the small GTPase superfamily regulate many aspects of cell behavior, including gene expression, cytoskeleton reorganization, and vesicle and nuclear–cytoplasmic transport. In this proteomic analysis, 132 entries were associated with GTPases including 104 that belong to the small GTPase family with an additional 28 linked to GTP exchange factors (GAP/GEF). Rab proteins are mainly involved in membrane trafficking. In *E. histolytica*, 102 genes encoding Rab small GTPases have been annotated [64]. Among all annotated Rabs, there are only a dozen of which their localization or function, or both have been demonstrated. Rab7, Rab5, Rab11, RabA, and RabB are involved in lysosome biogenesis, phagocytosis, cyst formation, and cargo secretion, respectively. In this work, we found representatives of these

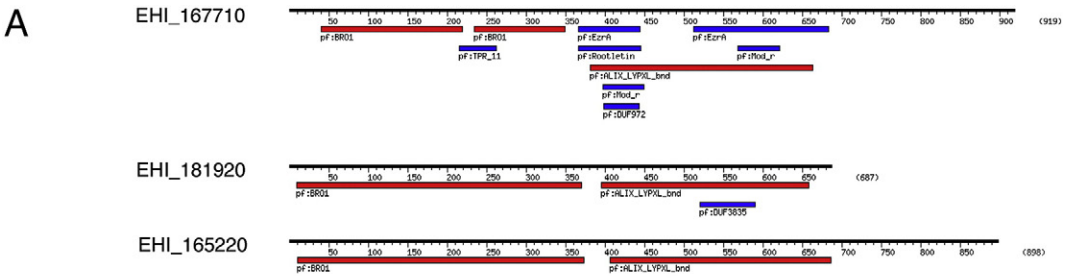

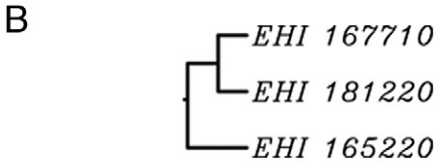

C

EHI_167710

```
1   MKINALPVLF QGDLYIASPV NLKVLRGCIQ QSNGDGIALQ KIDRMSELRV QCEDTTNGSL
61  NLLLEYDCLL AHLSQALLGA PLPIEFKWKI PITKKKTGLF SIIETTEVTL EEQSSSSINF
121 ERVHVLFNAG LITFRNATSL VSSIPTVPDS VKVFSKAAGI FVACIELADK CGLKKQSNDA
181 RLLSTISRGY AQLAMYVKAV NNNSSVMLRS KIAGGAVDLL RDGTKLLYNF ALIVAHNAAA
241 TVSEENLEYG DALSHYKECL KIIHESNNSK FEIMGKEIKS VFDSLMKDNN DIYMKPIPDV
301 TPEIQSRIVV TDTAYELKDQ ESPFKSIVPF ALRGPLQRYQ RESGKIVSDT KNDIPQYTVD
361 GDRVIQNINL RELENEVENL NGIPTRLRIV LSRIKGSNNI EEVLKQLEEM NEKNKKLRND
421 IEEINEELKE ESEENDMMRK KYQESWDRQP SNIVGREIYN EVEKISKILD FNKNCYLDGK
481 SLILKNELKI KILMKGEDEL INSLPKNNGS ILKEMVRQMT ELFESWNEIK VQREEAMNQI
541 IELQSKHQKT LLEEMKQASD KNIFIDSLIK EFVVHTNEIQ KNLNQQTELM NQIYTLHNDI
601 LQITTSVNGT KTSVCNEYSE IGEKYISKSL QIVEILVQLE SLEEDINKLQ KDVKKFCETR
661 KQELPIIEQR AKENIKKLDN ERKNQQPLQY SQNSYSTIPQ QYPPSFNPPP LQENNTSKPY
721 PSSYSSSYSQ NKNTTQYPSS YVTSQQQNNL TQYPSSYSPS NQLNNQPPSY PSSYTVSKSN
781 QPVNRYPTTQ TSPPSISVNS YHPSYTTTNL TQPPLYSQIP QYQNTQYNYS NSTIPLGTFQ
841 PPVPTLSSPT STLPPPTTST TYPLSAQELP LSRGTQPYLS SSVGRVQYGT VPPPLSPYGT
901 VPAPATPYHS PYPYGYNPF
```

Fig. 7 – *E. histolytica* proteins presenting a BRO1 domain and ALIX homology. (A) The diverse domains were retrieved from KEGG base orthologue analysis. (B) The orthologue relations are depicted as a tree. (C) Amino acid sequence of EHI_167710 where the peptides (underlined and in bold) used to prepare an anti-Alix specific antibody are highlighted.

diverse Rabs with the exception of Rab5, linked to phagosome biogenesis, a phenomenon which is not activated in these experiments. Other representatives of the large family of Rab GTPases were also identified.

3.2.8. Protein cargo candidates

Several previously identified proteins, which are involved in *E. histolytica* virulence, were associated with the internal membrane fractions. These mainly correspond to a few categories: peptidases, surface molecules, and calcium binding factors. We can argue that these are either residents within the vesicular compartments during multiple processes including post-translational modification (i.e. the Gal/GalNAc lectin during glycosylation), vesicular trafficking (i.e. the lysine and glutamic rich protein KERP1), or confined to specific compartments such as lysosomes (i.e. cysteine proteinases and their receptors or inhibitors). Calcium binding proteins such as grainin 1 and grainin 2 were found with high abundance. The global analysis of internal membrane fraction also identifies 446 proteins of unknown function, which according to this analysis changed their status from predicted to existent proteins.

3.3. *Cellular localization of newly identified factors representative of vesicular compartments*

Due to the originality of Alix (EHI_167710) as a potential marker of MVB and cell division compartments in *E. histolytica*, we took advantage of the divergences at amino acid sequences to raise a specific antibody (Fig. 7C). The protein was detected by immunoblotting as expected at a molecular mass of 104 kDa in the purified internal membrane fraction (Fig. 8A). Electron microscopy analysis of the isolated internal membrane fraction showed anti-Alix antibody labeling of some vesicles (Fig. 8B, black arrows). Using confocal microscopy, we localized the protein and observed the labeling to be dispersed in discrete dots throughout the cytoplasm with proximity to the plasma membrane inside the trophozoite and in vesicles near the division furrow of dividing trophozoites (Fig. 8C). In a similar manner, Alix has been detected during cytokinesis [65].

Interestingly, the retromer complex was in previous work found involved in the regulation of cysteine protease delivery to the phagosomes [63], signaling a secondary role to retromer complex and possibly a dual localization near the nuclei for protein traffic and near to the plasma membrane for dynamic vesicle trafficking functions. The known classical function of the retromer has been shown to shift toward a role in the recycling of surface receptors [66] and in the mitochondria–peroxisome transport pathway in mammalian cells [67], implying a plurality in this traffic structure.

4. Discussion

Cellular compartmentalization is an important evolutionary innovation, which sustains the functional specialization of cellular organelles. Membrane trafficking interconnects the nuclear envelope, endoplasmic reticulum, Golgi apparatus, and diverse secretory vesicles. These diverse compartments can be visualized by a variety of microscopy approaches. Membrane compartmentalization is extensively developed in eukaryotes including unicellular organisms such as *Dictyostelium discoideum*, the social amoeba. However, it is not the case for *E. histolytica*, a

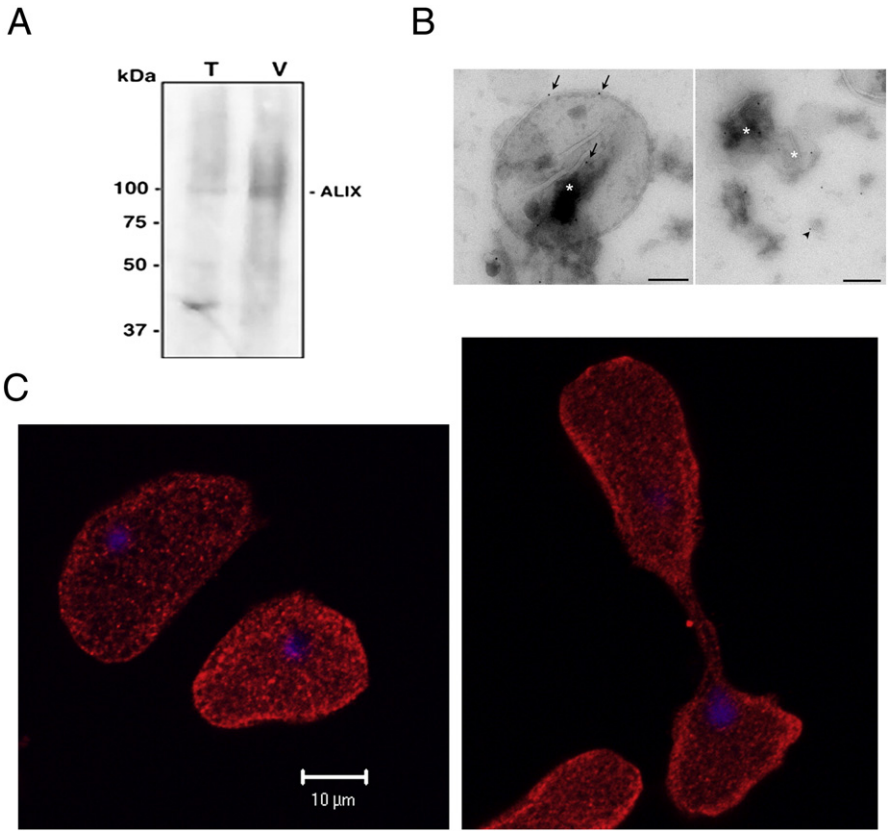

Fig. 8 – Cellular localization of. *E. histolytica* Alix-like protein. (A) An Alix-like protein with a molecular mass of 100 kDa was detected in the total protein extracts (T) and in the subcellular fractionation corresponding to vesicles (V). (B) The endomembrane fraction of trophozoites was adhered to EM grids and labeled with an antibody against Alix, followed by protein A gold (10 nm). The micrograph shows the presence of Alix (arrows) on the limiting membrane of a vacuole (white asterisk). Alix is also localized on smaller vacuoles (white asterisks) as well as to vesicles (black arrows). Scale bar = 200 nm. (C) Confocal imaging micrographs of *E. histolytica*. Trophozoites were labeled with anti-Alix antibody (red) and DAPI (blue). The image is taken from a focal plane at the middle of the cells showing Alix localized in small vesicles trough the cytoplasm, near the membrane region and in a dividing cell in vesicles close to the furrow. Scale bar = 10 µm.

pathogenic amoeba without mitochondria and in which a "bona fide" ER or Golgi is not clearly observable in electron microscopy, and indeed, these organelles have yet to be characterized. Numerous vesicles, vacuoles, and very few tiny stacks of membrane pairs can be observed in *E. histolytica* [68], which are expected to be essential for the secretion of pathogenic factors during infection of human organs. Bioinformatics analysis of data obtained from genome sequencing showed that *E. histolytica* possesses genes encoding important components necessary for the formation of structures or signaling pathways required for vesicular trafficking [14,69]. Specific studies then focused on protease transport toward the plasma membrane [63]. The observation of the Golgi collapse after Brefeldin A treatment [23] and ER fragmentation using nitric oxide [21] demonstrates the presence, functionality, and relevance of such organelles in *E. histolytica*. Using live cell imaging, the ER was found to be uniformly distributed in the cytoplasm while forming connecting structures [21]. This observation is different than what is expected in mammalian cells where ER appears concentrated in perinuclear areas. However, divergences are not unique to the ER, i.e. inhibition of Golgi function does not block or stop the traffic of de novo synthesized proteases, suggesting that alternative trafficking mechanisms are present in *E. histolytica* [23].

To gain insight into the endomembrane system of *E. histolytica*, we took advantage of proteomics applied to an amoebic fraction enriched for internal membranes. The analysis discovered, for the first time, important components of intracellular trafficking with strong iBAQ intensity values indicative of their abundance. The most abundant protein found in this analysis was calreticulin, which in *E. histolytica* is a resident of the ER (with expected calcium-buffering and chaperone functions) and has also been localized near to the plasma membrane during interaction with target cells and at phagocytic cups [53]. We then, carefully reviewed the significance of identified proteins with respect to their mammalian or yeast cell counterparts. The data confirmed that the principal participants for the TGN, ER to Golgi and plasma membrane trafficking are present in *E. histolytica*, although the morphology of these subcellular compartments is still not completely delineated. TGN and ER to Golgi network transport components were, in the majority, well identified. Both COPI and COPII subunits were accounted for, as well as NSF. The presence of the SNARE complex and SNARE interacting proteins for the fusion and abscission of vesicles were recognized. Also, the retromer complex (EhVps26-29 and -35) previously identified during phagocytosis [63], was detected and localized in non-phagocyting trophozoites analyzed here at the perinuclear region, in the cytoplasm and enriched at the plasma membrane. These findings support the existence of trans-Golgi network (TGN) components similar to the ones described in mammalian cells. However, cellular localization of markers for such networks like NSF and the retromer complex, suggest a peculiar compartmentalization of the TGN in *E. histolytica*. This hypothesis is reinforced by the absence of golgins, which are Golgi-resident proteins that form a matrix to help maintain the organelle structure. In contrast, the vast presence of GTPase, Rab, and Ras proteins in *E. histolytica* is suggestive of highly active membrane trafficking processes [70], vesicle formation, vesicle movement, and/or membrane fusion. Due to all these features, we consider that the multiple vesicles observed by electron microscopy in the parasite cytoplasm account, in part, for the morphological support of cargo transport.

Besides the ER components, the top two categories identified by LC–MS/MS correspond to endosomes and MVBs. The endosomal system in *E. histolytica*, necessary for the engulfment of external particles, is acidified with a delay [71]; therefore, it is not surprising to find a significant number of V-ATPases in our analysis. As for clathrin-coated pits, amoebic endosomes have been previously reported to be involved in the uptake of iron particles [55]. Here, we provide the first evidence that an established clathrin coated vesicle system for endocytosis exists in *E. histolytica*, with the majority of AP adaptors being present suggesting that the main components for such processes are in place. In the particular case of MVB components, the ESCRT complex (0, -I, -II, and -III) was previously described in *E. histolytica* with 20 genes encoding potential ESCRT orthologous including Vps4 (only one gene) and ADH112 adhesin (EHI_181220) with homology to Alix. Interestingly, endogenous Vps4 was localized to the cytoplasm in discrete dots, but when overexpressed, is enriched at the plasma membrane [28], suggesting dynamic roles for the ESCRT complex. In our analysis, we could not identify Vps4, however we did identify a novel orthologue of Alix (EHI_ 167710) that has multiple protein domains including BRO1. This Alix orthologue was localized at the plasma membrane and during cellular fission, and in purified vesicles as well. Relevantly, mammalian Alix plays a key role in ESCRT-mediated membrane abscission during cytokinesis and virus budding, participates in apoptosis and endocytosis and its N-terminal Bro1 domain recruits and/or regulates the membrane scission [58]. Until now there has not been a described amoebic Alix with similar observed functions such as those characterized for human cells or yeast. More relevant, in the closely related amoeba *Dictyostelium*, disruption of Alix encoding gene leads to a defect in differentiation by the impediment of relevant required receptor(s) to be located at the plasma membrane [72] indicating a preserved and fundamental role for Alix in the amoeba.

5. Conclusions

Overall, we have traveled through the endomembrane network of *E. histolytica*. This single-cell organism possesses the basic components to fulfill protein and cargo sorting. We have demonstrated the richness of vesicles and vacuoles present in the cytoplasm of *E. histolytica* and our findings support the importance of these structures in the dynamics of the endomembrane system, even more relevant by identification, detection, and localization of an Alix orthologue that could play a significant role at the plasma membrane of *E. histolytica* where most of the virulence factors have been detected. Pinpointing the basic actions in protein traffic and identifying components of cargo and vesicle sorting could shed some light on the process of virulence factor release, similar to the MBV pathway being a drug delivery target in *T. brucei* [73] and *Leishmania major* [74]. This is an important step missing in drug therapy development for *E. histolytica*.

Supplementary data to this article can be found online at http://dx.doi.org/10.1016/j.jprot.2014.07.034.

Conflict of interests

The authors declare that they have no competing interests.

Authors' contributions

NG conceived the study. DP and GDJ performed experiments and participated in its design. NA-A and SS performed experiments. MS performed electron microscopy studies. GDJ performed mass spectrometry analysis. DP, NA-A, GDJ, MS and NG wrote the manuscript. All authors read and approved the final manuscript.

Acknowledgments

The authors thank Pascal Roux (Imagopole, Pasteur) for assistance in image acquisition experiments. We acknowledge Sherri Smith for critical reading and correcting the manuscript.

This work is supported by grants to NG from the French National Agency for Research (ANR-10-INTB-1301-PARACTIN) and from the French parasitology network of excellence ParaFrap (Grant ANR-11-LABX0024). DP was supported by fellowships from the French Ministère de la Recherche et la Technologie (MRT) and from Fondation pour la Recherche Médicale (FRM). GDJ is supported by the Wellcome Trust–DBT India Alliance (Grant 500080/Z/09/Z).

REFERENCES

[1] Bannykh SI, Balch WE. Membrane dynamics at the endoplasmic reticulum–Golgi interface. J Cell Biol 1997;138:1–4.
[2] Malhotra V, Erlmann P. Protein export at the ER: loading big collagens into COPII carriers. EMBO J 2011;30:3475–80.
[3] Rambourg A, Clermont Y. Three-dimensional electron microscopy: structure of the Golgi apparatus. Eur J Cell Biol 1990;51:189–200.
[4] Preuss D, Mulholland J, Franzusoff A, Segev N, Botstein D. Characterization of the *Saccharomyces* Golgi complex through the cell cycle by immunoelectron microscopy. Mol Biol Cell 1992;3:789–803.
[5] Grunow A, Becker B, Melkonian M. Isolation and characterization of the Golgi apparatus of a flagellate scaly green alga. Eur J Cell Biol 1993;61:10–20.
[6] Yelinek JT, He CY, Warren G. Ultrastructural study of Golgi duplication in *Trypanosoma brucei*. Traffic 2009;10:300–6.
[7] Kondylis V, Rabouille C. The Golgi apparatus: lessons from *Drosophila*. FEBS Lett 2009;583:3827–38.
[8] Glick BS, Luini A. Models for Golgi traffic: a critical assessment. Cold Spring Harb Perspect Biol 2011;3:a005215.
[9] Lee C, Goldberg J. Structure of coatomer cage proteins and the relationship among COPI, COPII, and clathrin vesicle coats. Cell 2010;142:123–32.
[10] McNew JA, Parlati F, Fukuda R, Johnston RJ, Paz K, Paumet F, et al. Compartmental specificity of cellular membrane fusion encoded in SNARE proteins. Nature 2000;407:153–9.
[11] McMahon HT, Gallop JL. Membrane curvature and mechanisms of dynamic cell membrane remodelling. Nature 2005;438:590–6.
[12] Del Conte-Zerial P, Brusch L, Rink JC, Collinet C, Kalaidzidis Y, Zerial M, et al. Membrane identity and GTPase cascades regulated by toggle and cut-out switches. Mol Syst Biol 2008;4:206.
[13] Hughson FM, Reinisch KM. Structure and mechanism in membrane trafficking. Curr Opin Cell Biol 2010;22:454–60.
[14] Dacks JB, Davis LA, Sjogren AM, Andersson JO, Roger AJ, Doolittle WF. Evidence for Golgi bodies in proposed 'Golgi-lacking' lineages. Proc Biol Sci 2003;270(Suppl. 2):S168–71.
[15] Bredeston LM, Caffaro CE, Samuelson J, Hirschberg CB. Golgi and endoplasmic reticulum functions take place in different subcellular compartments of *Entamoeba histolytica*. J Biol Chem 2005;280:32168–76.
[16] Teixeira JE, Huston CD. Evidence of a continuous endoplasmic reticulum in the protozoan parasite *Entamoeba histolytica*. Eukaryot Cell 2008;7:1222–6.
[17] Mi-ichi F, Abu Yousuf M, Nakada-Tsukui K, Nozaki T. Mitosomes in *Entamoeba histolytica* contain a sulfate activation pathway. Proc Natl Acad Sci U S A 2009;106:21731–6.
[18] Girard-Misguich F, Sachse M, Santi-Rocca J, Guillen N. The endoplasmic reticulum chaperone calreticulin is recruited to the uropod during capping of surface receptors in *Entamoeba histolytica*. Mol Biochem Parasitol 2008;157:236–40.
[19] Gardai SJ, McPhillips KA, Frasch SC, Janssen WJ, Starefeldt A, Murphy-Ullrich JE, et al. Cell-surface calreticulin initiates clearance of viable or apoptotic cells through trans-activation of LRP on the phagocyte. Cell 2005;123:321–34.
[20] Ghosh SK, Field J, Frisardi M, Rosenthal B, Mai Z, Rogers R, et al. Chitinase secretion by encysting *Entamoeba invadens* and transfected *Entamoeba histolytica* trophozoites: localization of secretory vesicles, endoplasmic reticulum, and Golgi apparatus. Infect Immun 1999;67:3073–81.
[21] Santi-Rocca J, Smith S, Weber C, Pineda E, Hon CC, Saavedra E, et al. Endoplasmic reticulum stress-sensing mechanism is activated in *Entamoeba histolytica* upon treatment with nitric oxide. PLoS One 2012;7:e31777.
[22] Sanchez R, Saralegui A, Olivos-Garcia A, Scapolla C, Damonte G, Sanchez-Lopez R, et al. *Entamoeba histolytica*: intracellular distribution of the sec61alpha subunit of the secretory pathway and down-regulation by antisense peptide nucleic acids. Exp Parasitol 2005;109:241–51.
[23] Manning-Cela R, Marquez C, Franco E, Talamas-Rohana P, Meza I. BFA-sensitive and insensitive exocytic pathways in *Entamoeba histolytica* trophozoites: their relationship to pathogenesis. Cell Microbiol 2003;5:921–32.
[24] Libros-Ziv P, Villalobo E, Mirelman D. *Entamoeba histolytica*: identification and characterization of an N-ethylmaleimide sensitive fusion protein homologue. Exp Parasitol 2005;110:276–9.
[25] Clark CG, Alsmark UC, Tazreiter M, Saito-Nakano Y, Ali V, Marion S, et al. Structure and content of the *Entamoeba histolytica* genome. Adv Parasitol 2007;65:51–190.
[26] Nozaki T, Nakada-Tsukui K. Membrane trafficking as a virulence mechanism of the enteric protozoan parasite *Entamoeba histolytica*. Parasitol Res 2006;98:179–83.
[27] Nakada-Tsukui K, Okada H, Mitra BN, Nozaki T. Phosphatidylinositol-phosphates mediate cytoskeletal reorganization during phagocytosis via a unique modular protein consisting of RhoGEF/DH and FYVE domains in the parasitic protozoon *Entamoeba histolytica*. Cell Microbiol 2009;11:1471–91.
[28] Lopez-Reyes I, Garcia-Rivera G, Banuelos C, Herranz S, Vincent O, Lopez-Camarillo C, et al. Detection of the endosomal sorting complex required for transport in

Entamoeba histolytica and characterization of the EhVps4 protein. J Biomed Biotechnol 2010;2010:890674.
[29] Diamond LS. Axenic cultivation of *Entamoeba histolytica*. Science 1961;134:336–7.
[30] Aley SB, Scott WA, Cohn ZA. Isolation of the plasma membrane of *Entamoeba histolytica*. Arch Invest Med (Mex) 1980;11:41–5.
[31] Arya R, Mehra A, Bhattacharya S, Vishwakarma RA, Bhattacharya A. Biosynthesis of *Entamoeba histolytica* proteophosphoglycan in vitro. Mol Biochem Parasitol 2003; 126:1–8.
[32] Hohenberg H, Mannweiler K, Muller M. High-pressure freezing of cell suspensions in cellulose capillary tubes. J Microsc 1994;175:34–43.
[33] Wessel D, Flugge UI. A method for the quantitative recovery of protein in dilute solution in the presence of detergents and lipids. Anal Biochem 1984;138:141–3.
[34] Neuhauser N, Michalski A, Cox J, Mann M. Expert system for computer-assisted annotation of MS/MS spectra. Mol Cell Proteomics 2012;11:1500–9.
[35] Cox J, Mann M. MaxQuant enables high peptide identification rates, individualized p.p.b.-range mass accuracies and proteome-wide protein quantification. Nat Biotechnol 2008; 26:1367–72.
[36] Vizcaino JA, Cote RG, Csordas A, Dianes JA, Fabregat A, Foster JM, et al. The PRoteomics IDEntifications (PRIDE) database and associated tools: status in 2013. Nucleic Acids Res 2013; 41:D1063–9.
[37] Mayer A, Wickner W, Haas A. Sec18p (NSF)-driven release of Sec17p (alpha-SNAP) can precede docking and fusion of yeast vacuoles. Cell 1996;85:83–94.
[38] Seigneur M, Mounier J, Prevost MC, Guillen N. A lysine- and glutamic acid-rich protein, KERP1, from *Entamoeba histolytica* binds to human enterocytes. Cell Microbiol 2005; 7:569–79.
[39] Parsons HT, Christiansen K, Knierim B, Carroll A, Ito J, Batth TS, et al. Isolation and proteomic characterization of the *Arabidopsis* Golgi defines functional and novel components involved in plant cell wall biosynthesis. Plant Physiol 2012; 159:12–26.
[40] Anantharaman V, Aravind L. The GOLD domain, a novel protein module involved in Golgi function and secretion. Genome Biol 2002;3 [research0023].
[41] Clary DO, Griff IC, Rothman JE. SNAPs, a family of NSF attachment proteins involved in intracellular membrane fusion in animals and yeast. Cell 1990;61:709–21.
[42] Sutton RB, Fasshauer D, Jahn R, Brunger AT. Crystal structure of a SNARE complex involved in synaptic exocytosis at 2.4 Å resolution. Nature 1998;395:347–53.
[43] Rice LM, Brunger AT. Crystal structure of the vesicular transport protein Sec17: implications for SNAP function in SNARE complex disassembly. Mol Cell 1999;4:85–95.
[44] Bennett MK, Calakos N, Scheller RH. Syntaxin: a synaptic protein implicated in docking of synaptic vesicles at presynaptic active zones. Science 1992;257:255–9.
[45] Mallard F, Tang BL, Galli T, Tenza D, Saint-Pol A, Yue X, et al. Early/recycling endosomes-to-TGN transport involves two SNARE complexes and a Rab6 isoform. J Cell Biol 2002;156: 653–64.
[46] Amessou M, Fradagrada A, Falguieres T, Lord JM, Smith DC, Roberts LM, et al. Syntaxin 16 and syntaxin 5 are required for efficient retrograde transport of several exogenous and endogenous cargo proteins. J Cell Sci 2007;120:1457–68.
[47] Ganley IG, Espinosa E, Pfeffer SR. A syntaxin 10-SNARE complex distinguishes two distinct transport routes from endosomes to the trans-Golgi in human cells. J Cell Biol 2008; 180:159–72.
[48] Heider MR, Munson M. Exorcising the exocyst complex. Traffic 2012;13:898–907.
[49] Lobingier BT, Merz AJ. Sec1/Munc18 protein Vps33 binds to SNARE domains and the quaternary SNARE complex. Mol Biol Cell 2012;23:4611–22.
[50] Morgera F, Sallah MR, Dubuke ML, Gandhi P, Brewer DN, Carr CM, et al. Regulation of exocytosis by the exocyst subunit Sec6 and the SM protein Sec1. Mol Biol Cell 2012;23: 337–46.
[51] Munro S. The golgin coiled-coil proteins of the Golgi apparatus. Cold Spring Harb Perspect Biol 2011;3.
[52] Ohta E, Misumi Y, Sohda M, Fujiwara T, Yano A, Ikehara Y. Identification and characterization of GCP16, a novel acylated Golgi protein that interacts with GCP170. J Biol Chem 2003; 278:51957–67.
[53] Short B, Haas A, Barr FA. Golgins and GTPases, giving identity and structure to the Golgi apparatus. Biochim Biophys Acta 2005;1744:383–95.
[54] Field MC, Dacks JB. First and last ancestors: reconstructing evolution of the endomembrane system with ESCRTs, vesicle coat proteins, and nuclear pore complexes. Curr Opin Cell Biol 2009;21:4–13.
[55] Lopez-Soto F, Leon-Sicairos N, Reyes-Lopez M, Serrano-Luna J, Ordaz-Pichardo C, Pina-Vazquez C, et al. Use and endocytosis of iron-containing proteins by *Entamoeba histolytica* trophozoites. Infect Genet Evol 2009;9:1038–50.
[56] Wu M, Huang B, Graham M, Raimondi A, Heuser JE, Zhuang X, et al. Coupling between clathrin-dependent endocytic budding and F-BAR-dependent tubulation in a cell-free system. Nat Cell Biol 2010;12:902–8.
[57] Babst M. MVB vesicle formation: ESCRT-dependent, ESCRT-independent and everything in between. Curr Opin Cell Biol 2011;23:452–7.
[58] Ren X, Hurley JH. Proline-rich regions and motifs in trafficking: from ESCRT interaction to viral exploitation. Traffic 2011;12:1282–90.
[59] Moreno H, Linford AS, Gilchrist CA, Petri Jr WA. Phospholipid-binding protein EhC2A mediates calcium-dependent translocation of transcription factor URE3-BP to the plasma membrane of *Entamoeba histolytica*. Eukaryot Cell 2010;9:695–704.
[60] Garcia-Rivera G, Rodriguez MA, Ocadiz R, Martinez-Lopez MC, Arroyo R, Gonzalez-Robles A, et al. *Entamoeba histolytica*: a novel cysteine protease and an adhesin form the 112 kDa surface protein. Mol Microbiol 1999;33:556–68.
[61] Banuelos C, Garcia-Rivera G, Lopez-Reyes I, Orozco E. Functional characterization of EhADH112: an *Entamoeba histolytica* Bro1 domain-containing protein. Exp Parasitol 2005;110:292–7.
[62] Seaman MN. Recycle your receptors with retromer. Trends Cell Biol 2005;15:68–75.
[63] Nakada-Tsukui K, Saito-Nakano Y, Ali V, Nozaki T. A retromerlike complex is a novel Rab7 effector that is involved in the transport of the virulence factor cysteine protease in the enteric protozoan parasite *Entamoeba histolytica*. Mol Biol Cell 2005;16:5294–303.
[64] Nakada-Tsukui K, Saito-Nakano Y, Husain A, Nozaki T. Conservation and function of Rab small GTPases in *Entamoeba*: annotation of *E. invadens* Rab and its use for the understanding of *Entamoeba* biology. Exp Parasitol 2010;126: 337–47.
[65] Martin-Serrano J, Marsh M. ALIX catches HIV. Cell Host Microbe 2007;1:5–7.
[66] McGough IJ, Cullen PJ. Recent advances in retromer biology. Traffic 2011;12:963–71.
[67] Braschi E, Zunino R, McBride HM. MAPL is a new mitochondrial SUMO E3 ligase that regulates mitochondrial fission. EMBO Rep 2009;10:748–54.
[68] Mazzuco A, Benchimol M, De Souza W. Endoplasmic reticulum and Golgi-like elements in *Entamoeba*. Micron 1997; 28:241–7.

[69] Loftus B, Anderson I, Davies R, Alsmark UC, Samuelson J, Amedeo P, et al. The genome of the protist parasite *Entamoeba histolytica*. Nature 2005;433:865–8.
[70] Welter BH, Temesvari LA. Overexpression of a mutant form of EhRabA, a unique Rab GTPase of *Entamoeba histolytica*, alters endoplasmic reticulum morphology and localization of the Gal/GalNAc adherence lectin. Eukaryot Cell 2009;8:1014–26.
[71] Meza I, Clarke M. Dynamics of endocytic traffic of *Entamoeba histolytica* revealed by confocal microscopy and flow cytometry. Cell Motil Cytoskeleton 2004;59:215–26.
[72] Mattei S, Klein G, Satre M, Aubry L. Trafficking and developmental signaling: Alix at the crossroads. Eur J Cell Biol 2006;85:925–36.
[73] Kubata BK, Nagamune K, Murakami N, Merkel P, Kabututu Z, Martin SK, et al. Kola acuminata proanthocyanidins: a class of anti-trypanosomal compounds effective against *Trypanosoma brucei*. Int J Parasitol 2005;35:91–103.
[74] Zhang K, Showalter M, Revollo J, Hsu FF, Turk J, Beverley SM. Sphingolipids are essential for differentiation but not growth in *Leishmania*. EMBO J 2003;22:6016–26.